Int. J. Multiphase Flow Vol. 18, No. 5, pp. 705–726, 1992
Printed in Great Britain

0301-9322/92 $5.00 + 0.00
Pergamon Press Ltd

CRITERIA FOR THE TRANSITION FROM THE HOMOGENEOUS TO THE HETEROGENEOUS REGIME IN TWO-DIMENSIONAL BUBBLE COLUMN REACTORS

A. I. SHNIP,[1] R. V. KOLHATKAR,[2] D. SWAMY[2] and J. B. JOSHI[2]†

[1]Luikov Institute of Heat and Mass Transfer, Academy of Sciences, Minsk, Belarus

[2]Department of Chemical Technology, University of Bombay, Matunga Rd, Bombay 400 019, India

(Received 4 December 1991; in revised form 25 April 1992)

Abstract—Criteria have been developed for the prediction of the transition from the homogeneous to the heterogeneous regime in two-dimensional bubble columns. The theory of linear stability has been used for this purpose. Semibatch and continuous modes of operation have been analysed. The effects of sparger design, column height and the liquid phase physical properties have been investigated. A comparison between model predictions and experimental observations has been presented.

Key Words: bubble columns, homogeneous regime, heterogeneous regime, transition, bubbly flow, churn-turbulent flow

1. INTRODUCTION

In bubble columns, the gas phase exists as a dispersed phase in a continuous liquid phase. The gas phase moves in one of the two characteristic regimes, depending upon the nature of dispersion. The two regimes are: homogeneous and heterogeneous—and these are schematically shown in figure 1.

The homogeneous regime is also called the bubbly flow regime or quiescent bubbling regime and occurs at relatively low superficial gas velocities ($< \sim 50$ mm/s). This regime is characterized by almost uniformly sized bubbles. Further, the concentration of bubbles is uniform in the transverse direction. All the bubbles formed at the sparger rise virtually vertically if the bubble size is < 1–2 mm and larger bubbles rise with transverse and axial oscillations. For all sizes of bubbles, there is practically no coalescence or dispersion in the homogeneous regime. Hence the sizes of the bubbles are entirely dictated by the type and design of the sparger and the physical properties of the system.

During the bubble rise, some liquid is carried within the wakes of the bubbles. The liquid thus entrained is released when bubbles collapse at the top and flows downwards in the bubble-free region. In the case of small bubbles, which rise almost vertically, the liquid downflow is relatively well-defined. As a result, a liquid circulation pattern is developed. In the case of oscillating bubbles, well-directed liquid circulation does not exist. Indeed, turbulence is generated in the liquid phase because of the rapid changes in the path of the downflowing liquid. The liquid phase turbulence also arises due to the static pressure fluctuations resulting from the oscillating bubble motion. The feeble liquid circulation and the liquid phase turbulence both have the effect of decreasing the bubble rise velocity. The extent of the reduction increases with an increase in the bubble population (or the gas hold-up). This is the well-known hindrance effect. Due to the hindrance effect, the actual bubble rise velocity (V_B) in the homogeneous regime is less than the terminal rise velocity ($V_{B\infty}$). When all the bubbles rise with the terminal rise velocity, the fractional gas hold-up (ε_G) is given by the following equation:

$$\varepsilon_G = \frac{V_G}{V_{B\infty}}. \qquad [1a]$$

In the homogeneous regime, $V_B < V_{B\infty}$ and hence the slope of the ϵ_G vs V_G curve is $> (V_{B\infty})^{-1}$. The slope increases with an increase in the gas hold-up as shown by the line AB in figure 2.

†To whom correspondence should be addressed.

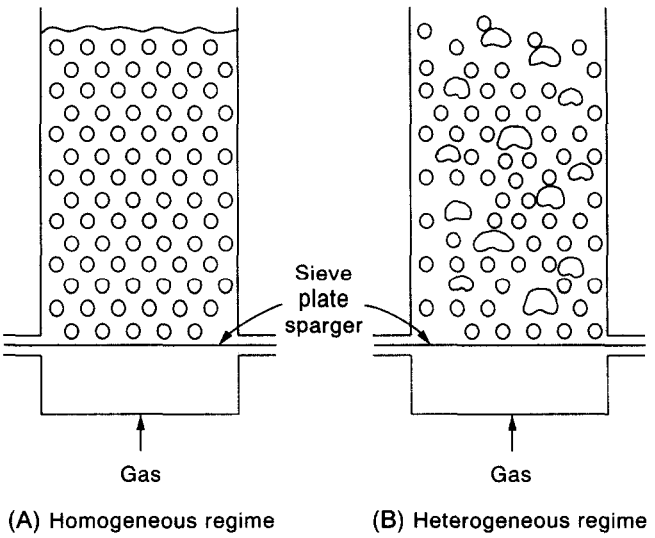

Figure 1. Schematic representation of the dispersion behaviour in the homogeneous and heterogeneous regimes.

The heterogeneous regime occurs at relatively high superficial gas velocities and is represented by the line DE in figure 2. This regime is characterized by the presence of a radial hold-up profile, as against a flat profile in the homogeneous regime. The maximum gas hold-up can occur at the column centre, as shown by Freedman & Davidson (1969), or near the column wall as shown in figures 3A and 3C, respectively.

The existence of the hold-up profile in the heterogeneous regime plays a dominant role. Because the gas density is negligible, the gas hold-up profile results into a profile of static pressure—as shown in figures 3A and 3C. This results in liquid circulation. For instance, in the case of the hold-up profile shown in figure 3A, the static pressure in the central region (such as at point B) is lower than the pressure in the near-wall region (such as at point A). As a consequence, liquid flow is generated from point A to point B, which continues in the upward direction in the central region up to point C. Flow reversal occurs at the top from point C to point D and the liquid flows in the downward direction near the column wall back to point A. The liquid circulation shown in figure 3D can be explained in a similar way.

The liquid circulation velocities are of the order of 0.3–3 m/s, depending upon the superficial gas velocity and the column dimensions. These liquid velocities are 1–2 orders of magnitude higher than

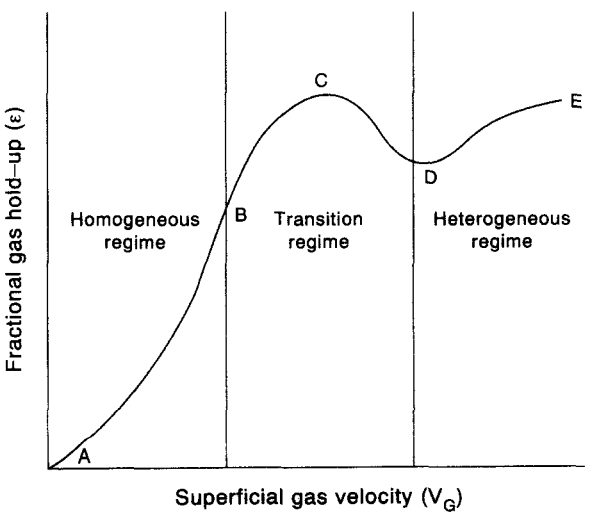

Figure 2. Schematic representation of the gas hold-up behaviour in the homogeneous transition and heterogeneous regimes.

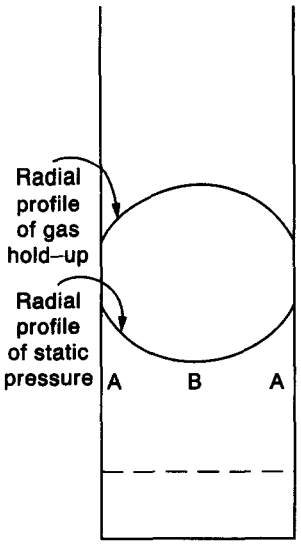

Figure 3A. Radial profiles of the gas hold-up and static pressure in the heterogeneous regime of a cylindrical bubble column.

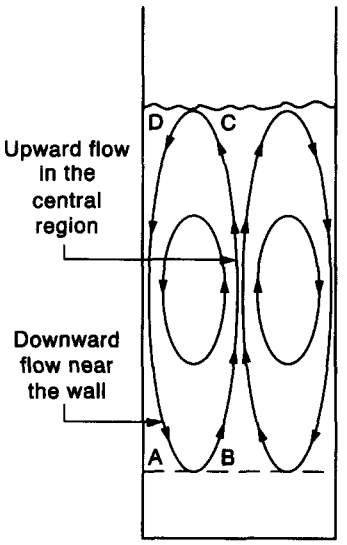

Figure 3B. Schematic representation of the liquid circulation in the heterogeneous regime of a cylindrical bubble column.

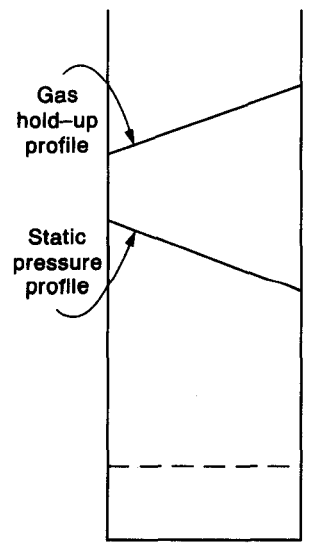

Figure 3C. Transverse profiles of the gas hold-up and static pressure in the heterogeneous regime of a two-dimensional bubble column.

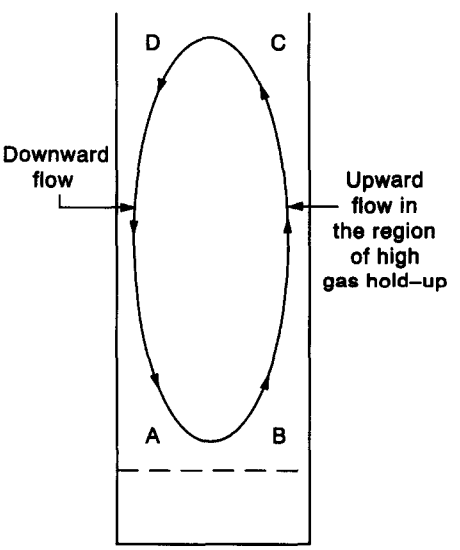

Figure 3D. Schematic representation of the liquid circulation in the heterogeneous regime of a two-dimensional bubble column.

the common range of superficial liquid velocities. Further, the intensity of turbulence is also much higher (3–5 times) than in single-phase pipe flows. Such a highly turbulent liquid circulation results in substantial enhancements in the values of the eddy diffusivities for mass, heat and momentum, as compared with the values in a single-phase pipe flow at the same superficial liquid velocity. As a result, the rates of heat and mass transfer and mixing are high in bubble columns. Therefore, a complete understanding of the internal circulation of the liquid is highly desirable for reliable and confident design of bubble columns.

The liquid circulation in the heterogeneous regime has a marked influence on the fractional gas hold-up. In the upflow region, the concentration of bubbles is higher than in the downflow region.

In this way, the liquid circulation provides a positive displacement to the gas phase in the upward direction. As a result, the average bubble rise velocity with respect to the column wall (V_0) is much higher than the terminal bubble rise velocity. Further, V_0 increases with an increase in the superficial gas velocity. Therefore, the fractional gas hold-up, which is given by

$$\varepsilon_G = \frac{V_G}{V_0}, \qquad [1b]$$

varies as V_G^n, where $n < 1$. This dependence is shown by the line DE in figure 2. It is pointed out again that $V_0 < V_{B\infty}$ is the homogeneous regime. Further, $n > 1$ in the homogeneous regime. In addition, the bubble size is fairly uniform in the homogeneous regime, whereas a wide bubble size distribution is observed in the heterogeneous regime. The bubble size continuously increases in the direction of increasing hold-up. The heterogeneous regime is spread over a much wider range of V_G when compared with the range of the homogeneous regime. Therefore, the heterogeneous regime is more commonly encountered in commercial columns.

The transition from the homogeneous to the heterogeneous regime occurs in the V_G range of B–D as shown in figure 2. In the homogeneous regime, gross liquid circulation is absent because of the flat hold-up profile. At a certain superficial gas velocity (point B), the onset of liquid circulation occurs. Once the circulation starts, more bubbles enter the upflow region, as compared with the downflow, as it is the path of lower resistance. As a result, a hold-up profile starts to build up, which in turn intensifies the liquid circulation. Thus, the build-up of the hold-up profile and the liquid circulation are self-propagating and occur simultaneously.

In the region B–C (figure 2), the liquid concentration is of small magnitude, though there is a noticeable change in the slope of the ε_G–V_G curve. In this region the effect of liquid circulation on the hold-up is small. However, in the range C–D, the rate of increase of the liquid circulation with respect to V_G is very pronounced. In other words, for a given change in V_G, the increase in the liquid circulation drives out bubbles at a faster rate than the rate of bubble generation. Therefore, the fractional gas hold-up decreases in the region CD. Nevertheless, the rate of decrease in ε_G reduces with an increase in V_G from C to D. At point D, the transition is complete and the heterogeneous regime begins. In this regime the liquid circulation velocity varies approximately as $V_G^{0.39}$. The rate of bubble generation is proportional to V_G. Therefore, the hold-up again starts increasing with V_G at point D, as shown in figure 2.

It is very important to note that the behaviour of bubble columns is markedly different in the homogeneous and heterogeneous regimes. The dependence of the rates of momentum, mass and heat transfer on the design and operating parameters [such as the column width (L), column height (H), superficial gas and liquid velocities (V_G and V_L), liquid density (ρ_L), liquid viscosity (μ_L) and the interfacial tension (σ)] is also substantially different in the homogeneous and heterogeneous regimes. Therefore, for the rational design it is important to know the range of parameters over which a particular regime prevails and the conditions under which the transition occurs.

In the past, some criteria have been developed for the transition on the basis of heuristic arguments. Joshi & Lali (1984) proposed that the transition will occur when the homogeneity of the dispersion is disturbed by the liquid phase turbulence. At the transition point, the r.m.s. fluctuating velocity of the liquid phase equals the bubble rise velocity. In the turbulent regime, the bubble motion is completely random because of liquid phase turbulence. Good agreement was shown between the model predictions and the experimental observations.

Ranade & Joshi (1987) have developed different criteria for small (<2 mm) and large (>2 mm) bubbles. The small bubbles rise upwards without any oscillations. The liquid carried upwards in the bubble wakes is released at the top liquid surface which then flows downwards. The downward liquid flow hinders the bubble rise. It was proposed that the transition will occur when the bubble rise velocity equals the downward velocity. Using the liquid phase mass balance and the wake volume given by Kumar & Kuloor (1972) (11/15 times the bubble volume), the following criterion was obtained:

$$\frac{\frac{11}{15}\varepsilon_{GC}}{1 - \varepsilon_{GC} - \frac{11}{15}\varepsilon_{GC}} = 1. \qquad [2]$$

The preceding equation predicts a transition value of 0.42 for small bubbles. The small bubbles are formed and preserved in a non-coalescing medium. This value is in agreement with the experimental findings of Oels *et al.* (1978), Maruyama *et al.* (1981) and Koetsier *et al.* (1976). It may be noted that the maximum possible hold-up is 0.52 using the cubic lattice structure.

The large bubbles rise with oscillations. The resulting oscillations in the gas hold-up generate liquid phase turbulence. The scale of turbulence in the homogeneous regime is $0.5d_B$ (Joshi 1983). Therefore, the possibility of bubble coalescence will increase when the distance between the bubbles is $<0.5d_B$. Using this value for bubble clearance and the cubic lattice structure, the value of the critical hold-up works out to be 0.16. This is in fairly good agreement with the experimental values of 0.15–0.2 reported by Deckwer (1977) and Whalley & Davidson (1974). It is to be noted out that Taitel *et al.* (1980) observed enhanced coalescence when $\varepsilon_G > 0.18$. This value also agrees favourably with the value of 0.16 proposed by Ranade & Joshi (1987).

Yamashita & Inoue (1975) and Maruyama *et al.* (1981) have reported experimental results on the transition gas velocity. These studies are useful for checking the validity of mathematical models. The aim of the present work is to develop a transition criterion in a two-dimensional bubble column on the basis of linear stability theory. The derivation of the stability criterion is presented in the next section, followed by a comparison with the experimental data on transition. The criterion is also extended for fluidized beds, including gas and liquid fluidized beds.

2. MATHEMATICAL MODEL

In this section a criterion is developed for the case of a two-dimensional bubble column. A schematic diagram of the column together with the coordinate system is shown in figure 4A.

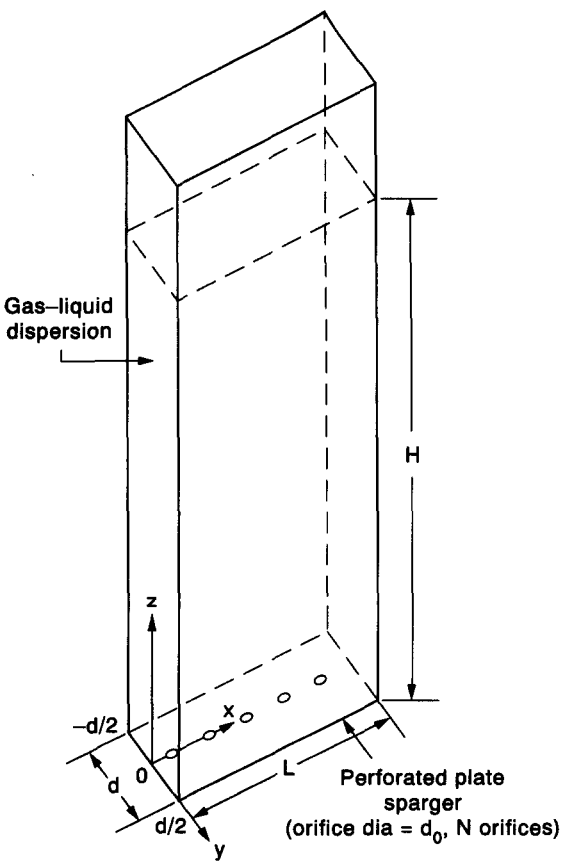

Figure 4A. Coordinate system for a two-dimensional bubble column.

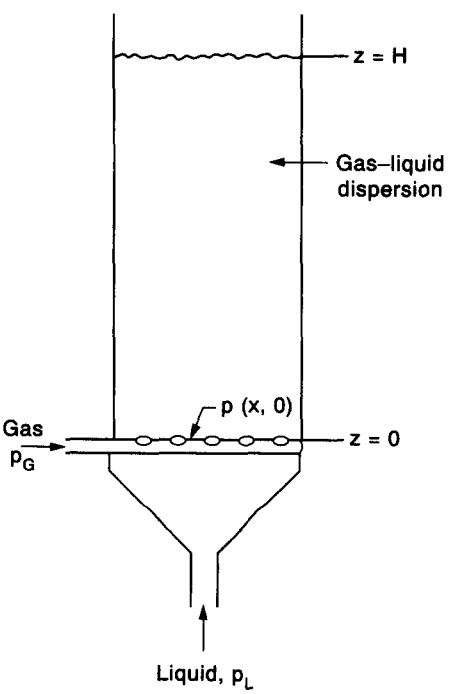

Figure 4B. Arrangement of the gas and liquid inlets.

Initially a model will be developed for the case of semibatch operation, where the gas phase is continuous and the liquid phase is batch. The following assumptions are made:

(1) The gas and liquid are considered as incompressible fluids, whereas the dispersion is considered compressible. The compressibility is accounted for by the spatial variation of the fractional gas hold-up, ε_G.
(2) The gas is massless.
(3) For simplicity, the liquid flow is considered to be laminar.

The continuity equation and the momentum balance for the liquid continuum are as follows:

$$\frac{\partial}{\partial t}\{\rho_L(1-\varepsilon_G)\} + \bar{\nabla}\cdot[\rho_L(1-\varepsilon_G)\bar{V}] = 0 \qquad [3a]$$

and

$$\rho_L(1-\varepsilon_G)\left[\frac{\partial \bar{V}}{\partial t} + (\bar{V}\cdot\bar{\nabla})\bar{V}\right] = -\varepsilon_L\bar{\nabla}p + \rho_L(1-\varepsilon_G)\bar{g} + \nabla\cdot\bar{\tau}_L + f\bar{e}_z, \qquad [3b]$$

where f is the interaction term and is given as

$$f = (1-\varepsilon_G)\varepsilon_G(\rho_L - \rho_G)g;$$

since for a gas–liquid system $\rho_G \ll \rho_L$, f can be approximated as

$$f = (1-\varepsilon_G)\varepsilon_G\rho_L g.$$

Similarly for the gas continuum, the continuity equation is as follows:

$$\frac{\partial \varepsilon_G}{\partial t} + \bar{\nabla}\cdot(\varepsilon_G \mathbf{V}_G) = 0, \qquad [3c]$$

where $\bar{V}$ and $\bar{V}_G$ are the velocity vectors for the liquid and gas phases, respectively, and ρ_L is the liquid density.

Gas bubbles are considered to be moving up in the vertical direction with a velocity $V_S(\varepsilon_G)$ relative to the liquid phase, thus:

$$\bar{V}_G = \bar{V} - V_S(\varepsilon_G)\frac{\bar{g}}{g}. \qquad [4]$$

For the two-dimensional column with the coordinate system shown in figure 4A, we have

$$\bar{V} = v\bar{e}_x + w\bar{e}_z \qquad [5a]$$

and

$$\bar{g} = -g\bar{e}_z \qquad [5b]$$

Further, we assume that $L \gg d$ and $H \gg d$. Substitution of [4] and [5] into [3a–c] gives:

$$\frac{\partial \varepsilon_G}{\partial t} + v\frac{\partial \varepsilon_G}{\partial x} + w\frac{\partial \varepsilon_G}{\partial z} - (1-\varepsilon_G)\left(\frac{\partial v}{\partial x} + \frac{\partial w}{\partial z}\right) = 0; \qquad [6]$$

x-component,

$$\rho_L(1-\varepsilon_G)\left(\frac{\partial v}{\partial t} + w\frac{\partial v}{\partial z} + v\frac{\partial v}{\partial x}\right) = -(1-\varepsilon_G)\frac{\partial p}{\partial x} + \mu\frac{\partial}{\partial x}\left\{2(1-\varepsilon_G)\frac{\partial v}{\partial x}\right\} + \mu\frac{\partial}{\partial y}\left\{(1-\varepsilon_G)\frac{\partial v}{\partial y}\right\}$$
$$+ \mu\frac{\partial}{\partial z}\left\{(1-\varepsilon_G)\left(\frac{\partial v}{\partial z} + \frac{\partial w}{\partial x}\right)\right\} - \tfrac{2}{3}\mu\frac{\partial}{\partial x}\left\{\frac{\partial}{\partial x}(1-\varepsilon_G)v + \frac{\partial}{\partial z}(1-\varepsilon_G)w\right\} \qquad [7]$$

and

z-component,

$$\rho_L(1-\varepsilon_G)\left(\frac{\partial w}{\partial t} + w\frac{\partial w}{\partial z} + v\frac{\partial w}{\partial x}\right) = -(1-\varepsilon_G)\frac{\partial p}{\partial z} - \rho_L(1-\varepsilon_G)g + f + \mu\frac{\partial}{\partial z}\left\{2(1-\varepsilon_G)\frac{\partial w}{\partial z}\right\}$$
$$+ \mu\frac{\partial}{\partial y}\left\{(1-\varepsilon_G)\frac{\partial w}{\partial y}\right\} + \mu\frac{\partial}{\partial x}\left\{(1-\varepsilon_G)\left(\frac{\partial v}{\partial z} + \frac{\partial w}{\partial z}\right)\right\} - \tfrac{2}{3}\mu\frac{\partial}{\partial z}\left\{\frac{\partial}{\partial x}(1-\varepsilon_G)v + \frac{\partial}{\partial z}(1-\varepsilon_G)w\right\}. \qquad [8]$$

Equation [3c] becomes

$$\frac{\partial \varepsilon_G}{\partial t} + v\frac{\partial \varepsilon_G}{\partial x} + (w + V_S + \varepsilon_G V_S')\frac{\partial \varepsilon_G}{\partial z} + \varepsilon_G\left(\frac{\partial v}{\partial x} + \frac{\partial w}{\partial z}\right) = 0, \quad [9]$$

where v and w are the components of the liquid velocity in the x- and z-directions, respectively, and $V_S' = dV_S/d\varepsilon_G$.

Now let us introduce the dimensionless variables defined below:

$$V = \frac{v}{V_{B\infty}}, \quad W = \frac{w}{V_{B\infty}}, \quad \bar{V}_S(\varepsilon_G) = \frac{V_S(\varepsilon_G)}{V_{B\infty}}, \quad Z = \frac{z}{L},$$

$$X = \frac{x}{L}, \quad h = \frac{H}{L}, \quad \tau = \frac{tV_{B\infty}}{L}, \quad \mathrm{Re} = \frac{LV_{B\infty}\rho_L}{\mu},$$

$$Y = \frac{y}{L}, \quad P = \frac{p}{\rho_L V_{B\infty}^2}, \quad G = \frac{gL}{V_{B\infty}^2}; \quad [10]$$

where $V_{B\infty} = V_S(\varepsilon_G = 0)$ and $\mu = \mu_M + \mu_T$ (μ_M and μ_T are the molecular and eddy viscosities, respectively).

Substitution of [10] in [6]–[9] results in the following dimensionless equations:

$$\frac{\partial \varepsilon_G}{\partial \tau} + V\frac{\partial \varepsilon_G}{\partial X} + W\frac{\partial \varepsilon_G}{\partial Z} + (1-\varepsilon_G)\left(\frac{\partial V}{\partial X} + \frac{\partial W}{\partial Z}\right) = 0, \quad [11]$$

$$(1-\varepsilon_G)\left(\frac{\partial V}{\partial \tau} + W\frac{\partial V}{\partial Z} + V\frac{\partial V}{\partial X}\right) = -(1-\varepsilon_G)\frac{\partial P}{\partial X} + \frac{1}{\mathrm{Re}}\left\{\frac{\partial}{\partial X}\left((1-\varepsilon_G)\frac{\partial V}{\partial X}\right)\right.$$
$$\left. + \frac{\partial}{\partial Y}\left((1-\varepsilon_G)\frac{\partial V}{\partial Y}\right) + \frac{\partial}{\partial Z}\left((1-\varepsilon_G)\frac{\partial V}{\partial Z}\right) + \frac{1}{3}\frac{\partial}{\partial X}\left(\frac{\partial}{\partial X}(1-\varepsilon_G)V + \frac{\partial}{\partial Z}(1-\varepsilon_G)W\right)\right\}, \quad [12]$$

$$(1-\varepsilon_G)\left(\frac{\partial W}{\partial \tau} + W\frac{\partial W}{\partial Z} + V\frac{\partial W}{\partial X}\right) = -(1-\varepsilon_G)\frac{\partial P}{\partial Z} + G(1-\varepsilon_G)^2 + \frac{1}{\mathrm{Re}}\left\{\frac{\partial}{\partial Z}\left((1-\varepsilon_G)\frac{\partial W}{\partial Z}\right)\right.$$
$$\left. + \frac{\partial}{\partial Y}\left((1-\varepsilon_G)\frac{\partial W}{\partial Y}\right) + \frac{\partial}{\partial X}\left((1-\varepsilon_G)\frac{\partial V}{\partial Z}\right) + \frac{1}{3}\frac{\partial}{\partial Z}\left(\frac{\partial}{\partial X}(1-\varepsilon_G)V + \frac{\partial}{\partial Z}(1-\varepsilon_G)W\right)\right\} \quad [13]$$

and

$$\frac{\partial \varepsilon_G}{\partial \tau} + V\frac{\partial \varepsilon_G}{\partial X} + [W + V_S + \varepsilon_G V_S'(\varepsilon_G)]\frac{\partial \varepsilon_G}{\partial Z} + \varepsilon_G\left(\frac{\partial V}{\partial X} + \frac{\partial W}{\partial Z}\right) = 0. \quad [14]$$

2.1. Hydrodynamic Stability Analysis for a Semibatch Bubble Column

Consider a rectangular column of width L and breadth d ($L \gg d$) having a perforated plate type of sparger (N orifices of diameter d_o each, the thickness of plate being l). Let the ratio of the column cross-sectional area to the gas sparging area be R. The pressure drop across the gas sparger is represented as the sum of the effect of both viscous and turbulent resistance to flow and is expressed as

$$p_G - p(X, 0) = k_V V_G + k_T V_G^2, \quad [15]$$

where p_G is the pressure below the sparger and $p(x, 0)$ is the pressure at the column bottom and above the sparger plate; k_V and k_T are the proportionality constants, V_G is the superficial gas velocity and is given by the following equation in the homogeneous regime:

$$V_G = V_S(\varepsilon_G)\varepsilon_G.$$

Let us introduce dimensionless variables as follows:

$$\bar{V}_G = \frac{V_G}{V_{B\infty}}, \quad K_V = \frac{k_v}{\rho_L V_{B\infty}}, \quad K_T = \frac{k_T}{\rho_L},$$

$$P_G = \frac{p_G}{\rho_L V_{B\infty}^2}, \quad P(X, 0) = \frac{p(X, 0)}{\rho_L V_{B\infty}^2}. \quad [16]$$

Therefore, [15] in dimensionless form becomes

$$P_G - P(X,0) = K_V \bar{V}_G + K_T \bar{V}_G^2. \quad [17]$$

As the terms accounting for viscous dissipation are negligible in comparison with the inertial terms, this is a potential flow problem and zero relative velocity conditions at the wall are redundant and only the conditions of zero normal velocity at the walls are used. The boundary conditions are:

$$X = 0, \quad V = 0; \quad [18.1]$$

$$X = 1, \quad V = 0; \quad [18.2]$$

$$Z = 0, \quad W = 0; \quad [18.3]$$

and

$$Z = h, \quad W = 0. \quad [18.4a]$$

Further, at $Z = 0$:

$$P_G - P(X,0) = K_V \bar{V}_G + K_T \bar{V}_G^2. \quad [18.4b]$$

According to the theory of hydrodynamic stability analysis, infinitesimally small perturbations are superimposed on the variables in the initial steady state and their transient behaviour is studied.

The variables in the perturbed state are as follows:

$$\varepsilon_G = \varepsilon_{G0} + \delta\varepsilon'_G, \quad [19.1]$$

$$V = V_0 + \delta V', \quad [19.2]$$

$$W = W_0 + \delta W' \quad [19.3]$$

and

$$P = P_0 + \delta P', \quad [19.4]$$

where δ is the smallness parameter.

The initial steady-state flow is the homogeneous flow regime (i.e. uniform bubbly flow regime) and is represented by the following equations:

$$V_0 = W_0 = 0, \quad [20.1]$$

$$\varepsilon_G(X, Y) = \varepsilon_{G0} = \text{const} \quad [20.2]$$

and

$$P(X,Z) = \frac{p_{atm}}{\rho_L V_{B\infty}^2} + G(h - Z)(1 - \varepsilon_{G0}) = P_0(X,Z). \quad [20.3]$$

Substituting [19.1]–[19.4] into [11]–[14] and retaining only those terms which are linear in δ, we get the following set of equations:

$$\frac{\partial \varepsilon'_G}{\partial \tau} + (1 - \varepsilon_{G0})\left(\frac{\partial V'}{\partial X} + \frac{\partial W'}{\partial Z}\right) = 0, \quad [21]$$

$$\frac{\partial \varepsilon'_G}{\partial \tau} + (V_S + \varepsilon_{G0} V'_S)\frac{\partial \varepsilon_G}{\partial Z} + \varepsilon_{G0}\left(\frac{\partial V'}{\partial X} + \frac{\partial W'}{\partial Z}\right) = 0, \quad [22]$$

$$(1 - \varepsilon_{G0})\frac{\partial V'}{\partial \tau} = -(1 - \varepsilon_{G0})\frac{\partial P'}{\partial X} + \frac{(1 - \varepsilon_{G0})}{Re}\left[\frac{\partial^2 V'}{\partial X^2} + \frac{\partial^2 V'}{\partial Y^2} + \frac{\partial^2 V'}{\partial Z^2} + \frac{1}{3}\frac{\partial}{\partial X}\left(\frac{\partial V'}{\partial X} + \frac{\partial V'}{\partial X}\right)\right] \quad [23]$$

and

$$(1 - \varepsilon_{G0})\frac{\partial W'}{\partial \tau} = -(1 - \varepsilon_{G0})\frac{\partial P'}{\partial Z} + \frac{(1 - \varepsilon_{G0})}{Re} \times \left[\frac{\partial^2 W'}{\partial X^2} + \frac{\partial^2 W'}{\partial Y^2} + \frac{\partial^2 W'}{\partial Z^2} + \frac{1}{3}\frac{\partial}{\partial Z}\left(\frac{\partial W'}{\partial X} + \frac{\partial W'}{\partial X}\right)\right] + 2G(1 - \varepsilon_{L0})\varepsilon'_G. \quad [24]$$

Since V and W have profiles in the y-direction, some averaging procedure will be employed for that direction.

As $L \gg d$ and $H \gg d$, the profiles of v and w in the y-direction can be represented as

$$V(x, y, z, t) = V_{\max}(x, z, t)\left(1 - \frac{2y}{d}\right)^n \quad [25a]$$

and

$$W(x, y, z, t) = W_{\max}(x, z, t)\left(1 - \frac{2y}{d}\right)^n, \quad [25b]$$

where $V_{\max}$ and $W_{\max}$ are the velocities in the central plane, $y = 0$. When the flow is turbulent n has the value of 1/7. The value of n can be selected to represent any other velocity profile, including viscous flow. It is emphasized, however, that the value of n is not important as far as the transition criterion is concerned. This aspect will be explained later.

The average values of these components can be obtained as

$$\bar{V}(x, z, t) = \frac{\int_{-d/2}^{d/2} V \, dy}{\int_{-d/2}^{d/2} dy} \quad [26a]$$

and

$$W(X, Z, \tau) = \frac{\int_{-d/2}^{d/2} W \, dY}{\int_{-d/2}^{d/2} dY}. \quad [26b]$$

Using [25a,b] and [26a,b] in [21]–[24], the momentum equations can be simplified to a great extent. Details of this simplification are given in Appendix A. The simplified equations are as follows:

$$\frac{\partial \varepsilon'_G}{\partial \tau} + (1 - \varepsilon_{G0})\left(\frac{\partial \bar{V}'}{\partial X} + \frac{\partial \bar{W}'}{\partial Z}\right) = 0, \quad [27]$$

$$\frac{\partial \varepsilon'_G}{\partial \tau} + (\bar{V}_S + \varepsilon_{G0}\bar{V}'_S)\frac{\partial \varepsilon_G}{\partial Z} + \varepsilon_{G0}\left(\frac{\partial \bar{V}'}{\partial X} + \frac{\partial \bar{W}'}{\partial Z}\right) = 0, \quad [28]$$

$$\frac{\partial \bar{V}'}{\partial \tau} = -\frac{\partial \bar{P}'}{\partial X} - \frac{\eta}{\mathrm{Re}}\bar{V}' \quad [29]$$

and

$$\frac{\partial \bar{W}}{\partial \tau} = -\frac{\partial \bar{P}'}{\partial Z} + 2G\varepsilon'_G - \frac{\eta}{\mathrm{Re}}\bar{W}'. \quad [30]$$

The solutions to [27]–[30] are represented in the following forms:

$$\bar{V}'(X, Z, \tau) = \bar{V}'(X, Z)e^{\lambda\tau}, \quad [31.1]$$

$$\bar{W}'(X, Z, \tau) = \bar{W}'(X, Z)e^{\lambda\tau}, \quad [31.2]$$

$$\bar{P}'(X, Z, \tau) = \bar{P}'(X, Z)e^{\lambda\tau} \quad [31.3]$$

and

$$\varepsilon'(X, Z, \tau) = \bar{\varepsilon}'_G(X, Z)e^{\lambda\tau}. \quad [31.4]$$

Substituting [31.1]–[31.4] in [27]–[30] and putting $\lambda = 0$ gives the equations determining the parameters at which the transition from the homogeneous to the heterogeneous regime occurs, these equations are called neutral motion equations and are as follows:

$$\frac{\partial \bar{V}'}{\partial X} + \frac{\partial \bar{W}'}{\partial Z} = 0, \quad [32]$$

$$(\bar{V}_S + \varepsilon_{G0}\bar{V}'_S)\frac{\partial \bar{\varepsilon}'_G}{\partial Z} + \varepsilon_{G0}\left(\frac{\partial \bar{V}'}{\partial X} + \frac{\partial \bar{W}'}{\partial z}\right) = 0, \quad [33]$$

$$\frac{\partial \bar{P}'}{\partial X} + \frac{\eta}{\mathrm{Re}} \bar{V}' = 0 \qquad [34]$$

and

$$\frac{\partial \bar{P}'}{\partial Z} - 2G\bar{\varepsilon}'_{\mathrm{G}} + \frac{\eta}{\mathrm{Re}} \bar{W}' = 0. \qquad [35]$$

The linearized boundary conditions for [32]–[35] are obtained using [18.1]–[18.4] in combination with [19.1]–[19.4] and retaining only those terms that are linear in δ. The boundary conditions are as follows:

$$X = 0, \qquad \bar{V}' = 0; \qquad [36.1]$$

$$X = 1, \qquad \bar{V}' = 0; \qquad [36.2]$$

$$Z = h, \qquad \bar{W}' = 0; \qquad [36.3]$$

$$Z = 0, \qquad \bar{W}' = 0; \qquad [36.4a]$$

and

$$Z = 0, \qquad \bar{\varepsilon}'_{\mathrm{G}} = -\frac{\beta}{\alpha} \bar{P}; \qquad [36.4b]$$

where

$$\alpha = \bar{V}_{\mathrm{S}} + \varepsilon_{\mathrm{G0}} \bar{V}'_{\mathrm{S}}$$

and

$$\beta = \frac{1}{K_{\mathrm{V}} + 2\varepsilon_{\mathrm{G0}} K_{\mathrm{T}} V_{\mathrm{S}}}.$$

Let us introduce the stream function Ψ, defined as follows:

$$\bar{V}' = -\frac{\partial \Psi}{\partial Z}, \quad \bar{W}' = \frac{\partial \Psi}{\partial X}. \qquad [37]$$

Combining [32], [33] and [37] we get

$$\alpha \frac{\partial \varepsilon_{\mathrm{G}}}{\partial Z} = 0; \qquad [38]$$

and combining [34], [35] and [37] we get

$$\frac{\eta}{\mathrm{Re}} \left(\frac{\partial^2 \Psi}{\partial X^2} + \frac{\partial^2 \Psi}{\partial Z^2} \right) - 2G \frac{\partial \bar{\varepsilon}'_{\mathrm{G}}}{\partial X} = 0. \qquad [39]$$

As $\alpha \neq 0$, from [38] we have

$$\frac{\partial \varepsilon''_{\mathrm{G}}}{\partial Z} = 0,$$

i.e.

$$\varepsilon'_{\mathrm{G}}(X, Z) = \bar{\varepsilon}'_{\mathrm{G}}(X, 0) \qquad [40]$$

or

$$\frac{\partial \bar{\varepsilon}'_{\mathrm{G}}(X, Z)}{\partial X} = \frac{\partial \bar{\varepsilon}'_{\mathrm{G}}(X, 0)}{\partial X}. \qquad [41]$$

Substitution of [36.4b] in [41] gives

$$\frac{\partial \varepsilon'_{\mathrm{G}}(X, Z)}{\partial X} = -\frac{\beta}{\alpha} \frac{\partial \bar{P}'(X, 0)}{\partial X}. \qquad [42]$$

Equation [34] at the boundary $(X, 0)$ takes the following form:

$$\frac{\partial \bar{P}'(X, 0)}{\partial X} = -\frac{\eta}{\mathrm{Re}} \bar{V}'(X, 0)$$

or

$$\frac{\partial \bar{P}'(X, 0)}{\partial X} = \frac{\eta}{\mathrm{Re}} \frac{\partial \Psi(X, 0)}{\partial z}. \qquad [43]$$

From [42] and [43], we get

$$\frac{\partial \bar{\varepsilon}'_G(X,Z)}{\partial Z} = -\frac{\beta}{\alpha}\frac{\eta}{\mathrm{Re}}\frac{\partial \Psi(X,0)}{\partial Z}. \qquad [44]$$

Substitution of [44] in [38] gives

$$\frac{\eta}{\mathrm{Re}}\left(\frac{\partial^2\Psi}{\partial X^2}+\frac{\partial^2\Psi}{\partial Z^2}\right)+2\frac{G\beta}{\alpha}\frac{\eta}{\mathrm{Re}}\frac{\partial\Psi(X,0)}{\partial Z}=0$$

or

$$\frac{\partial\Psi^2}{\partial X^2}+\frac{\partial\Psi^2}{\partial Z^2}+2\frac{G\beta}{\alpha}\frac{\partial\Psi(X,0)}{\partial Z}=0. \qquad [45]$$

Two points may be emphasized at this stage. First, is that the parameter η does not remain in [45]. It can be easily shown that the same result can be obtained even if [25a] were a parabolic profile, such as

$$V(X,Y,Z,\tau)=V_{\max}\left[1-\left(\frac{2Y}{d}\right)^2\right].$$

Secondly, the value of Re is also not important. Therefore, the values of the molecular (μ_M) and eddy viscosities (μ_T) are not important.

Equation [45], along with its boundary conditions, presents an eigenvalue problem for the parameter $A=(G\beta)/\alpha$. The lowest eigenvalue is the value at which the transition from the homogeneous to the heterogeneous regime occurs. Using the method of separation of variables, the final criterion is given as follows (details of the method are given in Appendix B):

$$2\frac{G\beta}{\alpha}=\frac{\pi\sinh(\pi h)}{\cosh(\pi h)-1}. \qquad [46]$$

The homogeneous regime would prevail as long as the left-hand side (LHS) of the above equation is less than the right-hand side (RHS) and the transition to the heterogeneous regime would occur as the LHS becomes greater than the RHS.

2.2. Stability Analysis for Continuous Operation

In this case, both the gas and the liquid are introduced and removed continuously. The flow of the two phases may occur in a cocurrent or countercurrent manner. Here the initial steady-state conditions are as follows:

$$\varepsilon_G=\varepsilon_{G0}=\text{const}, \qquad [47.1]$$

$$v=0, \qquad [47.2]$$

$$w=w_0=\text{const} \qquad [47.3]$$

and

$$P=P(Z)=\frac{p_{\text{atm}}}{\rho_L V_{B\infty}^2}+G(h-Z)(1-\varepsilon_{G0}), \qquad [47.4]$$

where w_0 is the true velocity of the liquid phase. The boundary condition at the bottom depends upon the way in which the liquid is introduced/taken away. Consider the bottom design given in figure 4B.

The liquid phase pressure drop consists of three parts: that due to the viscous and turbulent modes of friction across the sparger and that due to the acceleration of the liquid as it flows past the sparger region.

The liquid phase pressure drop can be written as follows:

$$p_L-p(x,0)=k_{VL}V_L+k_{TL}V_L^2+\left(\frac{\rho w^2}{Z}-\frac{\rho_L V_L^2}{Z}\right), \qquad [48]$$

where k_{VL} and k_{TL} are proportionality constants, $\rho=\rho_L(1-\varepsilon_G)$ is the dispersion density and V_L is the superficial velocity of the liquid in the column, where

$$V_L=w(1-\varepsilon_G).$$

Let us define the following dimensionless variables:

$$K_{VL} = \frac{k_{VL}}{\rho_L V_{B\infty}}, \quad K_{TL} = \frac{k_{TL} - \dfrac{\rho_L}{2}}{\rho_L}, \quad W = \frac{w}{V_{B\infty}}, \quad P_L = \frac{p_L}{\rho_L V_{B\infty}^2}. \tag{49}$$

Substitution of [49] into [48] gives

$$P_L - P(x, 0) = K_{VL} W(1 - \varepsilon_G) + W^2[K_{TL}(1 - \varepsilon_G)^2 + \tfrac{1}{2}(1 - \varepsilon_G)]. \tag{50}$$

In the perturbed state, the system variables are:

$$\varepsilon_G = \varepsilon_{G0} + \delta\varepsilon'_G, \tag{51.1}$$

$$V = \delta V', \tag{51.2}$$

$$W = W_0 + \delta W' \tag{51.3}$$

and

$$P = P_0 + \delta P'. \tag{51.4}$$

Substituting [51.1]–[51.4] in [11]–[14] and retaining only those terms which are linear in δ, we get the following linearized equations for perturbations. Further, averaging in the y-direction and following a procedure similar to the semibatch analysis we get the simplified linear equations as follows:

$$\frac{\partial\varepsilon'_G}{\partial\tau} + W_0\frac{\partial\varepsilon'_G}{\partial Z} - (1 - \varepsilon_{G0})\left(\frac{\partial\bar{V}'}{\partial X} + \frac{\partial\bar{W}'}{\partial Z}\right) = 0, \tag{52}$$

$$\frac{\partial\varepsilon'_G}{\partial\tau} + W_0\frac{\partial\varepsilon'_G}{\partial Z} + (\bar{V}_S + \varepsilon_{G0}\bar{V}_S)\frac{\partial\varepsilon'_G}{\partial Z} + \varepsilon_{G0}\left(\frac{\partial\bar{V}'}{\partial X} + \frac{\partial\bar{W}'}{\partial Z}\right) = 0, \tag{53}$$

$$\left[\frac{\partial\bar{V}'}{\partial\tau} + \frac{(n+1)^2}{(2n+1)}\bar{W}_0\frac{\partial\bar{V}'}{\partial Z}\right] = -\frac{\partial\bar{P}'}{\partial X} - \frac{\eta}{\mathrm{Re}}\bar{V}' \tag{54}$$

and

$$\left[\frac{\partial\bar{W}'}{\partial\tau} + \frac{(n+1)^2}{(2n+1)}\bar{W}_0\frac{\partial\bar{W}'}{\partial Z}\right] = -\frac{\partial\bar{P}'}{\partial Z} + 2G\varepsilon'_G - \frac{\eta}{\mathrm{Re}}\bar{W}'. \tag{55}$$

Substituting of [51.1]–[51.4] into [50] and linearization gives

$$\bar{P}' = \{K_{VL}(1 - \varepsilon_{G0}) + [K_{TL}(1 - \varepsilon_{G0})^2 + \tfrac{1}{2}(1 - \varepsilon_{G0})]\}\bar{W}' - [\bar{W}_0\{K_{VL} + \bar{W}_0[2K_{TL}(1 - \varepsilon_{G0}) + \tfrac{1}{2}]\}]\bar{\varepsilon}'_G. \tag{56}$$

The boundary condition for the gas sparger is the same as in the case of a semibatch bubble column; the linearized form of this is as follows:

$$-\bar{P}' = [K_V + 2K_T(\bar{W}_0 + \bar{V}_S)\varepsilon_{G0}](\bar{W}_0\bar{V}_S + \varepsilon_{G0}\bar{V}'_S)\bar{\varepsilon}'_G + \varepsilon_{G0}[K_V + K_T(\bar{W}_0 + \bar{V}_S)]\bar{W}'. \tag{57}$$

Let us define the following parameters:

$$B = \{K_{VL}(1 - \varepsilon_{G0}) + 2\bar{W}_0[K_{TL}(1 - \varepsilon_{G0})^2 + \tfrac{1}{2}(1 - \varepsilon_{G0})]\}^{-1}, \tag{58.1}$$

$$C = W_0\{K_{VL} + \bar{W}_0[2K_{TL}(1 - \varepsilon_{G0}) + \tfrac{1}{2}]\}, \tag{58.2}$$

$$E = \{[K_V + 2K_T(\bar{W}_0 + \bar{V}_S\varepsilon_{G0})](\bar{W}_0 + \bar{V}_S + \varepsilon_{G0}\bar{V}'_S)\} \tag{58.3}$$

and

$$F = [K_V + 2\varepsilon_{G0}K_T(W_0 + \bar{V}_S)]\varepsilon_{G0}. \tag{58.4}$$

Substitution of [58.1]–[58.4] into [56] and [57] gives

$$\bar{W}' = -B(\bar{P}' - C\bar{\varepsilon}'_G) \tag{59.1}$$

and

$$\bar{\varepsilon}'_G = -E(\bar{P}' + F\bar{W}'). \tag{59.2}$$

From [57.1] and [57.2] we have

$$\bar{W}' = -S\bar{P}' \tag{60}$$

and

$$\bar{\varepsilon}'_G = -Q\bar{P}', \tag{61}$$

where

$$S = \frac{B(1+EC)}{(1+BECF)}, \quad Q = \frac{E(1-BF)}{(1+BECF)}. \tag{62}$$

By using the normal mode of representation for all perturbation variables, as in [31.1]–[31.4], and putting $\lambda = 0$, we get the neutral motion equations as follows:

$$\frac{\partial \bar{V}'}{\partial X} + \frac{\partial \bar{W}'}{\partial Z} - \frac{\bar{W}_0}{(1-\varepsilon_{G0})}\frac{\partial \bar{\varepsilon}'_G}{\partial Z} = 0, \tag{63}$$

$$(W_0 + \bar{V}_S + \varepsilon_{G0}\bar{V}'_S)\frac{\partial \bar{\varepsilon}_G}{\partial Z} + \varepsilon_{G0}\left(\frac{\partial \bar{V}'}{\partial X} + \frac{\partial \bar{W}'}{\partial Z}\right) = 0, \tag{64}$$

$$\frac{(n+1)^2}{(2n+1)}\bar{W}_0\frac{\partial \bar{V}'}{\partial Z} = -\frac{\partial \bar{P}'}{\partial X} - \frac{\eta}{\mathrm{Re}}\bar{V}' \tag{65}$$

and

$$\frac{(n+1)^2}{(2n+1)}\bar{W}_0\frac{\partial \bar{W}'}{\partial Z} = -\frac{\partial \bar{P}'}{\partial Z} + 2G\,\bar{\varepsilon}'_G - \frac{\eta}{\mathrm{Re}}\bar{W}'. \tag{66}$$

The corresponding boundary conditions are as follows:

$$X = 0, \quad \bar{V}' = 0; \tag{67.1}$$

$$X = 1, \quad \bar{V}' = 0; \tag{67.2}$$

$$Z = h, \quad \bar{P}' = 0; \tag{67.3}$$

and

$$Z = 0, \quad \bar{W}' = -S\bar{P}, \quad \bar{V}' = 0, \quad \bar{\varepsilon}'_G = -Q\bar{P}'. \tag{67.4}$$

Equations [63] and [64] together give

$$\alpha_0\frac{\partial \bar{\varepsilon}'_G}{\partial Z} = 0, \tag{68}$$

where

$$\alpha_0 = \frac{\bar{W}_0}{(1-\varepsilon_{G0})} + \bar{V}_S + \varepsilon_{G0}\bar{V}'_S.$$

If $\alpha \neq 0$ then $\dfrac{\partial \bar{\varepsilon}'_G}{\partial Z} = 0$ and [63] becomes

$$\frac{\partial \bar{V}'}{\partial X} + \frac{\partial \bar{W}'}{\partial Z} = 0. \tag{69}$$

Introducing the stream function Ψ, we get

$$\sigma\frac{\partial}{\partial Z}\left(\frac{\partial^2\Psi}{\partial Z^2} + \frac{\partial^2\Psi}{\partial X^2}\right) + \frac{\eta}{\mathrm{Re}}\left(\frac{\partial^2\Psi}{\partial Z^2} + \frac{\partial^2\Psi}{\partial X^2}\right) + 2GQ\left(\sigma\frac{\partial^2\Psi}{\partial Z^2} + \frac{\eta}{\mathrm{Re}}\frac{\partial\Psi}{\partial Z}\right)_{z=0}, \tag{70}$$

where

$$\sigma = \frac{(n+1)^2}{(2n+1)}\bar{W}_0.$$

The boundary conditions for Ψ are:

$$X = 0, \quad \frac{\partial \Psi}{\partial Z} = 0; \tag{71.1}$$

$$X = 1, \quad \frac{\partial \Psi}{\partial Z} = 0; \tag{71.2}$$

$$Z = h, \quad \sigma \frac{\partial^2 \Psi}{\partial Z^2} + \frac{\eta}{\mathrm{Re}} \frac{\partial \Psi}{\partial Z} = 0; \tag{71.3}$$

and

$$Z = 0, \quad \begin{bmatrix} \dfrac{\partial^2 \Psi}{\partial X^2} = -Q\left(\sigma \dfrac{\partial^2 \Psi}{\partial Z^2} + \dfrac{\eta}{\mathrm{Re}} \dfrac{\partial \Psi}{\partial Z}\right) \\ \dfrac{\partial \Psi}{\partial Z} = 0 \end{bmatrix}. \tag{71.4}$$

Let us define

$$\Phi = \sigma \frac{\partial \Psi}{\partial Z} + \frac{\eta}{\mathrm{Re}} \Psi. \tag{72}$$

Equation [72] suggests the following form for Ψ:

$$\Psi = \exp\left(-\frac{\eta Z}{\mathrm{Re}\,\sigma}\right)\left[\int_0^z \frac{1}{\sigma} \exp\left(\frac{\eta Z}{\mathrm{Re}\,\sigma}\right)\Phi \, \mathrm{d}Z + c\right]. \tag{73}$$

Equation [73] along with the boundary conditions [71.1]–[71.4] provides an eigenvalue problem. Proceeding in a manner similar to section 2.1 we obtain the criterion for transition for different modes. The earliest transition occurs for the lowest value of n, i.e. $n = 1$, and thus we have the stability criterion:

$$2GQ - \frac{\eta}{\mathrm{Re}} S = \pi \coth(\pi h). \tag{74}$$

As in the case of semibatch operation, the regime would be homogeneous as long as the LHS of the above equation is less than the RHS and a transition to the heterogeneous regime would occur when the LHS becomes greater than the RHS. Two special cases can be considered here.

Case 1

The pressure drop across the liquid sparger is very much less than that caused by its acceleration over the gas sparger region. This case corresponds to the situation when the column is connected at its bottom to a huge reservoir of liquid. Mathematically this can be written as

$$k_{\mathrm{VL}} \bar{V}_{\mathrm{L}} + k_{\mathrm{TL}} \bar{V}_{\mathrm{L}}^2 \ll \left(\frac{\rho w}{2} - \frac{\rho_{\mathrm{L}} \bar{V}_{\mathrm{L}}}{2}\right). \tag{75}$$

Under limiting conditions this means that, $k_{\mathrm{VL}} \to 0$ and $k_{\mathrm{TL}} \to 0$ and the parameters B and C are defined as follows:

$$B = \frac{1}{W_0 \varepsilon_{\mathrm{G0}}(1 - \varepsilon_{\mathrm{G0}})}, \quad C' \bar{W}_0^2 (\varepsilon_{\mathrm{G0}} - \tfrac{1}{2}). \tag{76}$$

The parameters E and F are defined as in [58.3] and [58.4]. The stability criterion is given by [74].

Case 2

The pressure drop across the liquid sparger is sufficiently large to ensure uniform liquid flow into the column, irrespective of the pressure perturbations in the column. Mathematically this means that

$$k_{\mathrm{VL}} \bar{V}_{\mathrm{L}} + k_{\mathrm{TK}} \bar{V}_{\mathrm{L}}^2 \gg \left(\frac{\rho w}{2} - \frac{\rho_{\mathrm{L}} \bar{V}_{\mathrm{L}}}{2}\right). \tag{77}$$

Under these limiting conditions, we have

$$k_{VL} \to \infty \quad \text{and} \quad k_{TL} \to \infty. \tag{78a}$$

Also,

$$W'(x, 0) = 0, \quad \text{hence } S = 0. \tag{78b}$$

Using the above conditions in [58.1], [58.2] and [62], we get

$$B \to 0, \quad C \to \infty, \quad \text{therefore } Q = E.$$

Under these conditions, the stability criterion becomes as follows:

$$G\{[K_V + 2K_T\varepsilon_{G0}(\bar{W}_0 + \bar{V}_S)](\bar{W}_0 + \bar{V}_S + \varepsilon_{G0}\bar{V}')\}^{-1} = \pi \coth(\pi h). \tag{79}$$

2.3. Estimation of the Model Parameters

In order to use the stability criterion developed in the previous section, we need to know the values of the pressure drop across the sparger and the bubble relative velocity.

2.3.1. Estimation of the relative velocity

The relative velocity is defined by the following equation:

$$V_S = \frac{V_G}{\varepsilon_G} - \frac{V_L}{\varepsilon_L}. \tag{80}$$

The value of the relative velocity is less than the terminal velocity. Richardson & Zaki (1954) have reported the following relationship between V_S and $V_{B\infty}$:

$$V_S(\varepsilon_G) = V_{B\infty}(1 - \varepsilon_G)^m. \tag{81}$$

The terminal rise velocity, $V_{B\infty}$ was estimated using the correlations given by Clift *et al.* (1978). The bubble size (formed at the orifice, d_B) was estimated using the correlation developed by Kumar & Kuloor (1972).

2.3.2. Estimation of the pressure drop across the gas sparger

The pressure drop across the gas sparger is expressed as follows:

$$\Delta P = k_V V_G + k_T V_G^2. \tag{82}$$

The two terms on the RHS represent the contributions due to the viscous and turbulent flow resistances.

In order to estimate the values of k_V and k_T in [82], the pressure drop was measured in a 155 × 10 × 1000 mm two-dimensional column. A perforated plate was used as a sparger with a single row of holes. The superficial gas velocity was varied in the range 10–100 mm/s. The hole diameter and the number of holes were varied in the range 0.5–2 mm and 5–15, respectively, so as to obtain the area ratio (column cross-sectional area to hole area) in the range 100–2000. The clear liquid height in the column was 500 mm. The pressure drop across the sparger was measured by subtracting the hydrostatic liquid head from the observed total pressure drop. The thickness of the sparger plate was found to have no influence on the pressure drop. The following correlation were obtained with a standard deviation of 5%:

$$k_V = 0.98R^{1.5} \tag{83}$$

and

$$k_T = 0.30R^2. \tag{84}$$

3. RESULTS AND DISCUSSION

3.1. Discussion on the Mathematical Model

The superficial gas velocity (V_{GC}) at which the transition from the homogeneous to the heterogeneous flow regime occurs depends mainly on the design of the gas sparger and the physical

properties of the system. In order to understand the effect of the above parameters on V_{GC}, plots were constructed on the basis of the stability criterion, [46]. The effects of the number of orifices, the orifice diameter, the bubble rise velocity and the gas hold-up index on V_{GC} were studied. In the case of continuous operation, the effect of the superficial liquid velocity on ε_{GC} and V_{GC} was studied. While studying the effect of the orifice diameter and the contribution of the viscous flow resistance on ε_{GC} and V_{GC}, the gas hold-up index was taken as 1.4.

3.1.1. Semibatch operation

The stability criterion is given by the following equation:

$$2\frac{G\beta}{\alpha} = \frac{\pi \sinh(\pi h)}{\cosh(\pi h) - 1}, \qquad [85]$$

where

$$G = \frac{gL}{V_{B\infty}^2}, \qquad [86]$$

$$\alpha = \bar{V}_S + \varepsilon_{G0}\bar{V}_S \qquad [87]$$

and

$$\beta = \frac{1}{K_V + 2\varepsilon_{G0}K_T V_S}. \qquad [88]$$

As discussed in section 2.1, a homogeneous flow regime can be maintained as long as the LHS of [85] is less than the RHS. For the aspect ratio ($h = H/L$) > 1, the RHS is a constant quantity. The LHS depends upon the design of the gas sparger and the physical properties of the liquid. The role of these parameters will not be discussed systematically.

Effect of sparger resistance. The sparger resistance is represented by [83] and [84]. The sparger resistance increases with an increase in the area ratio (R). The effect of the area ratio on ε_{GC} is shown in figure 5. It can be seen that ε_{GC} increases with an increase in R up to about 600 and then ε_{GC} levels off. The limiting value of ε_{GC} can be obtained as $R \to \infty$. Under these conditions k_V and $k_T \to \infty$ and hence $\beta \to 0$. In order to keep the RHS of [85] finite, α should tend to zero. With this condition, we get

$$\varepsilon_{GC} = \frac{1}{m+1}. \qquad [89]$$

For a typical value of $m = 1.4$ (Richardson & Zaki 1954), the value of ε_{GC} works out to be 0.42. In the published literature, the maximum value of the hold-up ($V_L = 0$) has been reported by Oels *et al.* (1978) and is in the range 0.42–0.48. The experimental value agrees favourably with the limiting value predicted by [89].

The effect of the area ratio on the transition gas velocity V_{GC} is shown in figure 6. It can be seen that the value of V_{GC} increases with an increase in the area ratio.

The effect of the hole sized d_o on ε_{GC} and V_{GC} is shown in figures 5 and 6, respectively. It can be seen that the values of ε_{GC} and V_{GC} decrease with an increase in d_o.

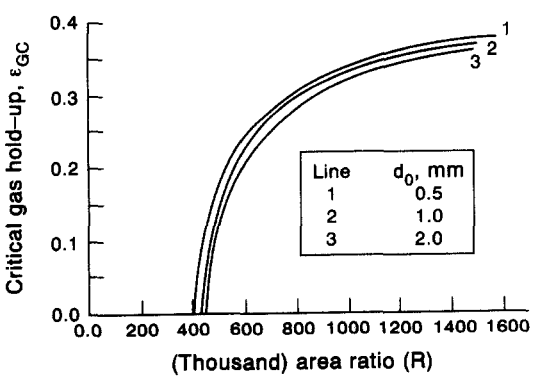

Figure 5. Effect of the sparger design on the critical gas hold-up for transition.

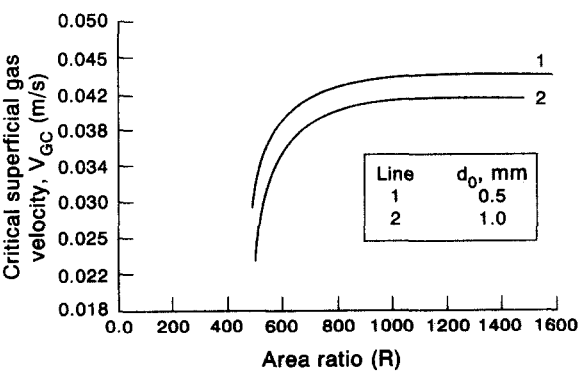

Figure 6. Effect of the sparger design on the critical superficial gas velocity for transition.

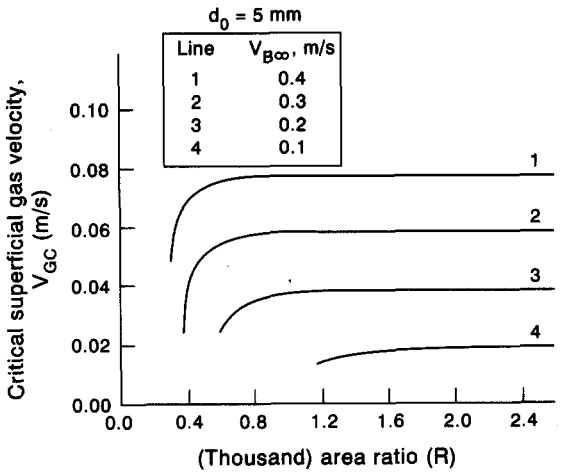

Figure 7. Effect of the bubble rise velocity on the critical superficial gas velocity for transition.

Effect of the bubble rise velocity. Liquid viscosity, surface tension and the liquid density govern the bubble rise velocity. It was thought desirable to study the effects of physical properties through the value of $V_{B\infty}$. The relationship between physical properties and bubble size has been given by Kumar & Kuloor (1972) and the relationship between physical properties and the bubble rise velocity (for a given size) has been given by Clift *et al.* (1978).

The effect of the bubble rise velocity on V_{GC} is shown in figure 7. It can be seen that the value of V_{GC} increases with an increase in $V_{B\infty}$.

Effect of the hold-up parameter. It was discussed in the introduction that the actual bubble rise velocity is lower than the terminal value and this hindrance effect increases with an increase in the gas hold-up. With the hindrance effect, the relationship between the superficial gas velocity and the fractional gas hold-up is

$$\frac{V_G}{V_{B\infty}} = \varepsilon_G(1-\varepsilon_G)^m. \qquad [90]$$

The hold-up parameter m depends upon the bubble Reynolds number. The effect of m on V_{GC} is shown in figures 8(A) and (B) for hole diameters of 0.5 and 1.5 mm, respectively. It can be seen that at a constant R the value of V_{GC} increases with a decrease in m.

3.1.2. *Continuous operation*

The liquid flow is either cocurrent or countercurrent to the gas flow. Liquid is introduced with the help of a distributor. Two limiting cases of the distributor resistance (k_{VL}) are considered: $k_{VL} = \infty$ and $k_{VL} = 0$. For the first case, the stability criterion is given by [79]. Substitution for λ_{11} gives

$$2G\{[K_V + 2K_T(W_0 + \bar{V}_S)\varepsilon_{G0}](W_0 + \bar{V}_S + \varepsilon_{G0}\bar{V}_S')\}^{-1} = 7.74\cosh(7.74h). \qquad [91]$$

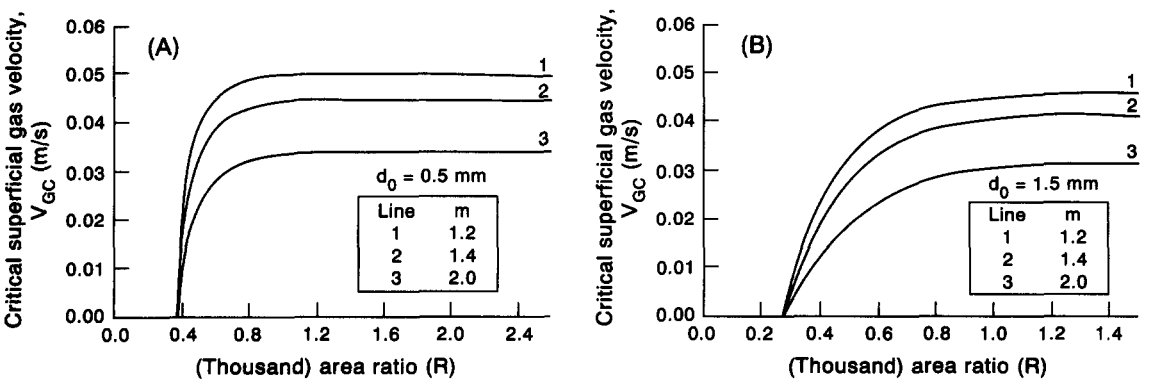

Figure 8. Effect of the hold-up parameter on the critical superficial gas velocity for transition.

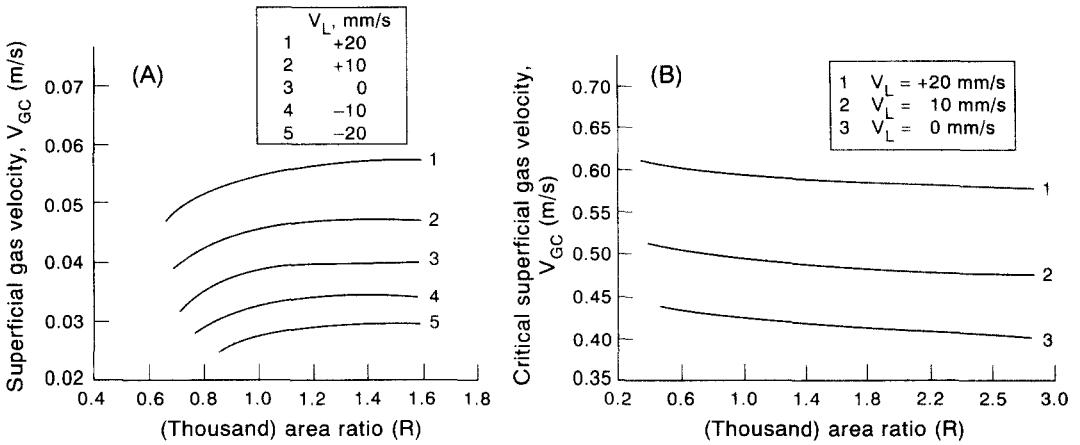

Figure 9. Effect of cocurrent and countercurrent liquid velocity on the critical superficial gas velocity for transition: (A) infinite resistance of the liquid phase sparger; (B) zero resistance of the liquid phase sparger.

The results are shown in figure 9(A) for cocurrent ($V_L = +10$ and $+25$ mm/s) and countercurrent (-10 and -25 mm/s) flows. It can be seen that the value of V_{GC} increases with an increase in the cocurrent liquid velocity, whereas, it decreases with an increase in the countercurrent liquid velocity. These predictions agree with the experimental observations of Oels *et al.* (1978).

The effect of liquid velocity can be qualitatively explained as follows. In the heterogeneous regime, liquid circulation is developed which is upward in the central region and downward in the annular region. With cocurrent liquid upflow the downward annular flow is restricted, resulting in a reduction in the liquid circulation. Therefore, the cocurrent liquid flow delays the transition. This countercurrent liquid flow has the opposite effect.

When the liquid distributor resistance is zero ($k_{VL} = 0$), the results are shown in figure 9(B). In this case also, the transition is delayed with an increase in the cocurrent V_L. However, the increase in V_{GC} is less for the case of $k_{VL} = 0$ as compared to the case of $k_{VL} = \infty$. When $k_{VL} = 0$, the disturbances at the bottom grow because of the absence of the possible dampening effect of the liquid distributor. For this case, the homogeneous regime is not possible when the liquid flow is countercurrent.

3.2. Comparison with Experimental Data

Yamashita & Inoue (1975), Maruyama *et al.* (1981) and Chisti (1989) have measured the values of the critical superficial gas velocity for transition. The details pertaining to the experiments are given in table 1. The comparison between the model predictions and experimental observations is shown in table 2. It can be seen that the agreement is favourable over a wide range of column width, hole diameter and number of holes.

It has been pointed out earlier that the maximum possible hold-up in the homogeneous regime is 42%. This prediction compares favourably with the experimental observations of Maruyama *et al.* (1981) and Koetsier *et al.* (1976).

In the case of fluidized beds, the particles of commercial importance and systems which have been studied employ particles which are <0.1 mm. In these cases, the sparger resistance can be

Table 1. Details of the reported experimental data (system: air–water)

	Column Column dimensions					
Investigator(s)	*L* (m)	*d* (m)	*H* (m)	Orifice dia (mm)	*N* or (area ratio)	Sparger thickness (mm)
Chisti (1989)	0.46	0.155	1.5	1	50 (1915)	2
Maruyama *et al.* (1981)	0.3	0.01	0.2 to 0.6	0.2	29 (3921)	20
Yamashita & Inoue (1975)	0.3	0.01	1.07	0.3	29 (1463)	0.7
	0.3	0.01	1.07	0.5	29 (527)	0.7

Table 2. Comparison between the model predictions and experimental observations (system: air–water)

Investigator(s)	N or (area ratio)	V_{GC}(mm/s) Reported value	V_{GC}(mm/s) Predicted value
Chisti (1989)	50(1815)	63.4	52.2
Maruyama *et al.* (1981)	29(3921)	39.1	46.6
Yamashita & Inoue (1975)	29(1463)	50	46.6
	29(527)	44	44

assumed to be infinite, and the limiting case defined by [89] can be assumed to hold good for these systems. In the case of fluidized beds, the limiting case is given as

$$\varepsilon_s = \frac{1}{m}, \qquad [92]$$

where ε_s is the particle phase hold-up and m is the Richardson–Zaki index. Tables 3A and 3B show the comparison for liquid and gas fluidized beds, respectively.

3.3. General Remarks

1. From figures 5–9 it can be seen that the value of V_{GC} increases with an increase in the area ratio. The area ratio increases either by decreasing the hole diameter or decreasing the number of holes. In figures 5–9, increasing R generally means a reduction in the hole diameter. A reduction in the number of holes may result in uneven sparging. Under these conditions, the gas jets issuing from the holes may create a local circulation pattern which can grow to result in the heterogeneous regime. Under the limiting condition of a single hole, it is known that the homogeneous regime cannot be observed—even at very low superficial gas velocities.
2. The transition also depends upon the coalescing behaviour of the liquid phase. Any coalescence will result in a higher local hold-up and generate local liquid circulation. Such a disturbance can grow to give the heterogeneous regime. The coalescence also results in higher bubble rise velocities and the value of ε_{GC} will be lower, even though the value of V_{GC} remains the same. This particular situation was observed in many studies reported in the literature.

Table 3A. Comparison of experimental data with the model predictions (bounded bed analysis); liquid fluidized systems (Gibilaro *et al.* 1986)

d_P (μm)	ρ_s (kg/m^3)	ρ_L (kg/m^3)	$\mu_L \times 10^{-3}$ (Pa-s)	ϵ^a_{mb} Expt	ϵ^a_{mb} Predict.
165	8710	1000	1.25	0.74	0.726
165	8710	1000	0.75	0.66	0.676
82.5	8710	1000	1.25	0.75	0.742
82.5	8710	1000	0.75	0.72	0.734

[a]Voidage at which the transition occurs.

Table 3B. Comparison of experimental data with the model predictions (bounded bed analysis); gas fluidized systems

d_p (mm)	ρ_s (kg/m^3)	ρ_G (kg/m^3)	$\mu_G \times 10^{-5}$ (Pa-s)	ϵ^a_{mb} Expt	ϵ^a_{mb} Predict.
		(i) Jacob & Wiemer (1987)			
44	850	14.20	1.66	0.765	0.752
44	850	42.61	1.66	0.767	0.761
44	850	71.01	1.66	0.798	0.782
		(ii) Mutsers & Rietama (1977)			
39.7	920	1.167	1.8	0.776	0.782
78	920	1.167	1.8	0.742	0.765
103	920	1.167	1.8	0.701	0.732

[a]Voidage at which the transition occurs.

4. CONCLUSIONS

(1) The transition from the homogeneous to the heterogeneous regime occurs when the conditions given by the following expressions are satisfied:

semibatch operation,

$$\frac{\frac{gL}{V_{B\infty}^2}}{(K_V + 2\varepsilon_{G0}K_T\bar{V}_S)(1-\varepsilon_{G0})^{m-1}[1-(m+1)\varepsilon_{G0}]} < \frac{\pi \sinh(\pi h)}{\cosh(\pi h)-1};$$

continuous operation,

$$\frac{\frac{gL}{V_{B\infty}^2}}{[K_V + 2\varepsilon_{G0}K_T(W_0+\bar{V}_S)](W_0+V_S+\varepsilon_{G0}\bar{V}_S')} < \pi \coth(\pi h).$$

(2) Good agreement was observed between the predicted and experimental values of the critical gas velocity over a wide range of hole diameter and the number of holes. Further, the maximum value of the predicted critical gas hold-up was 0.42, which agrees favourably with the experimental observation.
(3) Cocurrent liquid flow delays the transition, whereas countercurrent flow promotes an early transition. These predictions are known to agree with the experimental observations. However, experimental data are needed for two-dimensional columns.
(4) The transition criterion was found to be independent of the viscosity.

REFERENCES

CHISTI, M. Y. 1989 *Airlift Bioreactors*. Elsevier, New York.

CLIFT, R., GRACE, J. R. & WEBER, M. E. 1978 *Bubbles Drops & Particles*. Academic Press, New York.

DECKWER, W. D. 1977 Absorption and reaction of isobutene in sulfuric acid—III. Considerations on the scale up of bubble columns. *Chem. Engng Sci.* **32,** 51.

FREEDMAN, W. & DAVIDSON, J. F. 1969 Hold-up and liquid circulation in bubble columns. *Trans. Instn Chem. Engrs* **47,** T251–262.

GIBILARO, L. G., HOISSAIN, I. & FOSCOLO, P. U. 1986 Aggregative behaviour of liquid fluidized beds. *Can. J. Chem. Engng* **64,** 93.

JACOB, K. V. & WIEMER, A. W. 1987 High pressure particulate expansion and minimum bubbling of fine carbon powders. *AIChE Jl* **33,** 1698.

JOSHI, J. B. 1983 Solid–liquid fluidized beds—some design aspects. *Chem. Engng Res. Des.* **61,** 143–161.

JOSHI, J. B. & LALI, A. M. 1984 Velocity hold-up relationships in multiphase contactors. In *Frontiers in Chemical Reaction Engineering*, Vol. 2 (Edited by DORAISWAMY, L. K. & MASHELKAR, R. A.), p. 381. Wiley Eastern, New York.

KOETSIER, W. T., VAN SWAAIJ, W. P. M. & VAN DER MOST, M. J. 1976 Maximum gas hold-up in bubble columns. *J. Chem. Engng Japan* **9,** 332.

KUMAR, R. & KULOOR, N. R. 1972 *Formation of Bubbles and Drops*, Vol. 8 (Edited by DREW, T. B. *et al.*). Academic Press, New York.

MARUYAMA, T., YOSHIDA, S & MIZUSHINA, T. 1981 The flow transition in a bubble column. *J. Chem. Engng Japan* **14,** 352.

MOLERUS, O. & KURTIN, M. 1985 Hydrodynamics of bubble columns in the uniform bubbling regime. *Chem. Engng Sci.* **40,** 647.

MUTSERS, S. M. P. & RIETAMA, K. 1977 The effect of interparticle forces on the expansion of a homogeneous fluidized bed. *Powder Technol.* **18,** 239.

OELS, U., LUCKE, M., BUCHOLZ, R. & SCHUGERL, K. 1978 Influence of gas distributior type and composition of liquid on the behaviour of a bubble column bioreactor. *Ger. Chem. Engng* **1,** 115.

RANADE, V. V. & JOSHI, J. B. 1987 Transport phenomena in multiphase systems: momentum, mass and heat transfer in bubble column reactors. In *Transport Processes in Multiphase Systems* (Edited by UPADHYAY, S. N.), p. 113. Banaras Hindu Univ., Varanasi, India.

RICHARDSON, J. F. & ZAKI, W. N. 1954 Sedimentation and fluidisation. Part III: the sedimentation of uniform fine particles and of two-component mixtures of solids. *Trans. Instn Chem. Engrs* **39,** 348.

TAITEL, Y., BARNEA, D. & DUKLER, A. E. 1980 Modelling flow pattern transitions for steady upward gas–liquid flow in vertical tubes. *AIChE Jl* **26,** 345–354.

WHALLEY, P. B. & DAVIDSON, J. F. 1974 Liquid circulation in bubble columns. *Instn Chem. Engrs Symp. Ser.* **38,** J5.

YAMASHITA, F. & INOUE, H. 1975 Gas hold-up in bubble columns. *J. Chem. Engng Japan* **8,** 334.

APPENDIX A

Substitution of [26a, b] in [25a, b] gives

$$V(X, Y, Z, \tau) = \frac{n+1}{z^n}\,\bar{V}(X, Z, \tau)\left(1 - \frac{2Y}{d}\right)^n \qquad [A.1a]$$

and

$$W(X, Y, Z, \tau) = \frac{n+1}{z^n}\,\bar{W}(X, Z, \tau)\left(1 - \frac{2Y}{d}\right)^n. \qquad [A.1b]$$

This averaging in the y-direction also holds for the perturbation variables. Now, substituting [A.1a, b] in [21]–[24] and integrating each term w.r.t. Y from $-d/2$ to $d/2$ (assuming that the value of ε_G does not depend on y) and dividing throughout by d, we get the following equations:

$$\frac{\partial \varepsilon'_G}{\partial \tau} + (1 - \varepsilon_{G0})\left(\frac{\partial \bar{V}'}{\partial X} + \frac{\partial \bar{W}'}{\partial Z}\right) = 0, \qquad [A.2]$$

$$\frac{\partial \varepsilon'_G}{\partial \tau} + (\bar{V}_S + \varepsilon_{G0}\bar{V}'_S)\frac{\partial \varepsilon_G}{\partial Z} + \varepsilon_{G0}\left(\frac{\partial \bar{V}'}{\partial X} + \frac{\partial \bar{W}'}{\partial Z}\right) = 0, \qquad [A.3]$$

$$(1 - \varepsilon_{G0})\frac{\partial \bar{V}'}{\partial \tau} = -(1 - \varepsilon_{G0})\frac{\partial \bar{P}'}{\partial X} + \frac{(1 - \varepsilon_{G0})}{\mathrm{Re}}\left[\frac{\partial^2 \bar{V}'}{\partial X^2} + \eta \bar{V}'\frac{\partial^2 \bar{V}'}{\partial Z^2} + \frac{1}{3}\frac{\partial}{\partial X}\left(\frac{\partial \bar{V}'}{\partial X} + \frac{\partial \bar{V}'}{\partial X}\right)\right] \qquad [A.4]$$

and

$$(1 - \varepsilon_{G0})\frac{\partial \bar{W}'}{\partial \tau} = -(1 - \varepsilon_{G0})\frac{\partial \bar{P}'}{\partial Z} + \frac{(1 - \varepsilon_{G0})}{\mathrm{Re}} \times \left[\frac{\partial^2 \bar{W}'}{\partial X^2} + \eta \bar{W}'\frac{\partial^2 \bar{W}'}{\partial Z^2} + \frac{1}{3}\frac{\partial}{\partial Z}\left(\frac{\partial \bar{W}'}{\partial X} + \frac{\partial \bar{W}'}{\partial X}\right)\right] + 2G(1 - \varepsilon_{L0})\varepsilon'_L, \qquad [A.5]$$

where η is given by

$$\eta = \frac{n(n+1)L^2}{d^2}. \qquad [A.6]$$

Since $L \gg d$ and $H \gg d$ and for a typical value of $n = 1/7$ and $|\eta| \gg 1$, we have

$$|\eta \bar{V}'| \gg \frac{\partial^2 \bar{V}'}{\partial X^2} + \frac{\partial^2 \bar{V}'}{\partial Z^2} + \frac{1}{3}\frac{\partial}{\partial Z}\left(\frac{\partial \bar{V}'}{\partial X} + \frac{\partial \bar{W}'}{\partial Z}\right)$$

and

$$|\eta \bar{W}'| \gg \frac{\partial^2 \bar{W}'}{\partial X^2} + \frac{\partial^2 \bar{W}'}{\partial Z^2} + \frac{1}{3}\frac{\partial}{\partial Z}\left(\frac{\partial \bar{V}'}{\partial X} + \frac{\partial \bar{W}'}{\partial Z}\right).$$

As a result of this simplification [A.4] and [A.5] take the following form:

$$\frac{\partial \bar{V}'}{\partial \tau} = -\frac{\partial \bar{P}'}{\partial X} - \frac{\eta}{\mathrm{Re}}\bar{V}' \qquad [A.7]$$

and

$$\frac{\partial \bar{W}'}{\partial \tau} = -\frac{\partial \bar{P}'}{\partial Z} + 2G\varepsilon'_G - \frac{\eta}{\mathrm{Re}}\bar{W}'. \qquad [A.8]$$

APPENDIX B

Let us assume the following form for Ψ:

$$\Psi(X, Z) = \mathbf{X}(X) \cdot \mathbf{Z}(Z). \tag{B.1}$$

Using [B.1] in [45], we get

$$\frac{d^2\mathbf{X}}{dX^2} = -\lambda_1^2 \mathbf{X} \tag{B.2}$$

and

$$\frac{d^2\mathbf{Z}}{dZ^2} - \lambda_1^2 \mathbf{Z} = -D, \tag{B.3}$$

where λ_1 is a constant of separation and D is given by

$$D = 2\frac{G\beta}{\alpha}\frac{d\mathbf{Z}(0)}{dZ}.$$

The boundary conditions for [B.2] and [B.3] are:

$$X = 0, \quad \mathbf{X} = 0; \tag{B.4.1}$$

$$X = 1, \quad \mathbf{X} = 0; \tag{B.4.2}$$

$$Z = h, \quad \mathbf{Z} = 0; \tag{B.4.3}$$

and

$$Z = 0, \quad \mathbf{Z} = 0. \tag{B.4.4}$$

The general solution of [B.1] is

$$\mathbf{X} = C_1 \sin(\lambda_1 X) + C_2 \cos(\lambda_1 X).$$

To satisfy boundary condition [B.4.1],

$$C_2 = 0.$$

Further, to satisfy boundary condition [B.4.2]

$$\lambda_1 = \lambda_{1n} = n\pi (n = 0, 1, 2, 3, \ldots .)$$

The general solution of [B.3] is

$$\mathbf{Z}(Z) = A \sinh(n\pi Z) + B \cosh(n\pi Z) + \frac{D}{(n\pi)^2}. \tag{B.5}$$

Using boundary conditions [B.4.3] and [B.4.4] we get

$$A_n = \frac{n\pi \sinh(n\pi h)}{\cosh(n\pi h) - 1}. \tag{B.6}$$

The transition occurs at the lowest value of A_n (i.e. $n = 1$), and we have the criterion for transition as

$$2\frac{G\beta}{\alpha} = \frac{\pi \sinh(\pi h)}{\cosh(\pi h) - 1}. \tag{B.7}$$